Deep-Sea Research II 55 (2008) 1334–1347

Contents lists available at ScienceDirect

Deep-Sea Research II

journal homepage: www.elsevier.com/locate/dsr2

Microbial dynamics in cyclonic and anticyclonic mode-water eddies in the northwestern Sargasso Sea

Courtney S. Ewart [a], Meredith K. Meyers [a,b], Elisa R. Wallner [a], Dennis J. McGillicuddy Jr.[c], Craig A. Carlson [a,*]

[a] Marine Science Institute, University of California, Mail Code 9610, Santa Barbara, CA 93106-9610, USA
[b] Institute of Ecology, University of Georgia, Athens, GA 30602-2202, USA
[c] Woods Hole Oceanographic Institution, Woods Hole, MA 02543-1541, USA

ARTICLE INFO

Article history:
Accepted 26 February 2008
Available online 12 May 2008

Keywords:
Bacterioplankton
Bacterial production
Picoplankton
Mesoscale eddies
North Atlantic subtropical gyre
Sargasso Sea

ABSTRACT

The EDdy Dynamics, mixing, Export, and Species composition (EDDIES) project provided a unique opportunity to evaluate the response of the microbial community and further understand the biological and biogeochemical consequences of mesoscale perturbation events in an oligotrophic system. In order to characterize microbial dynamics, we performed measurements of bacterial biomass (BB) and production (BP) and phytoplankton pigment analyses in two upwelling eddies in the Sargasso Sea sampled in 2004 and 2005. We also observed a 3-fold increase in BP at the Bermuda Atlantic Time-series Study (BATS) site during the passage of a cyclonic eddy in 2003. Although the integrated BB and BP over 140 m in 2004 and 2005 eddies remained within the climatological range measured at the BATS site, there was systematic variability in bacterioplankton dynamics across both eddies. Cyclonic eddy C1 demonstrated decreased BP at the feature's center relative to its periphery, and BP was not correlated with total chlorophyll *a* (TChl *a*) variability. However, BP correlated with prymnesiophyte pigments throughout the feature. In contrast, mode-water eddy A4 showed an enhancement in BP at the eddy center (EC) relative to its edges and was coincident with elevated TChl *a*, high primary production measurements, and a high concentration of diatoms. In eddy A4, the tight relationship between enhanced BP, TChl *a* and specific phytoplankton taxa implies that the phytoplankton community structure was an important factor influencing BP variability. While the heterotrophic bacterial response in C1 and A4 was not enhanced relative to BATS summer climatology, these data and the presence of similar nutrient fields across both eddies suggest that BP and BB were influenced by the eddy perturbations and responded to changes in the phytoplankton community.

1. Introduction

Traditional mechanisms of nutrient supply, such as winter mixing, do not provide enough nutrients to the euphotic zone to balance geochemical estimates of new production in the oligotrophic regions such as the Sargasso Sea (Jenkins and Goldman, 1985). Eddy pumping has been proposed as an important mechanism of nutrient supply to the surface of the open sea (Falkowski et al., 1991; McGillicuddy et al., 1998; Siegel et al., 1999). In a cyclonic eddy, both the seasonal and permanent thermocline shoal, causing a negative sea-level anomaly (SLA) (McGillicuddy et al., 1999). In a mode-water eddy, the seasonal thermocline is uplifted while the permanent thermocline is depressed, leading to a positive SLA. Both types of eddies can lift isopycnals into the euphotic zone, injecting nutrients into nutrient-depleted surface waters that can be rapidly utilized, resulting in the accumulation of phytoplankton biomass and organic matter (McGillicuddy et al., 1998). The Sargasso Sea is characterized by the relatively frequent passage of eddies, which introduces spatial and temporal variability in the productivity of the North Atlantic subtropical gyre (Sweeney et al., 2003).

Eddies have been shown to enhance nutrient input to the surface ocean, resulting in increases in chlorophyll concentrations (McGillicuddy et al., 1998; Tarran et al., 2001) as well as new production (Falkowski et al., 1991; Harris et al., 1997; Oschlies and Garçon, 1998; Moran et al., 2001). For example, total chlorophyll *a* (TChl *a*) was enhanced in a cyclonic eddy sampled in the Algerian Basin (SW Mediterranean) and was coincident with 2–3-fold enhancement in primary production rates (Moran et al., 2001). In the NE Atlantic, a cyclonic cold-core eddy demonstrated high concentrations of TChl *a* and phytoplankton biomass (Lochte and Pfannkuche, 1987). Another cyclonic eddy in this same region

* Corresponding author. Tel.: +1 805 893 2541; fax: +1 805 893 8062.
E-mail address: carlson@lifesci.ucsb.edu (C.A. Carlson).

0967-0645/$ - see front matter © 2008 Elsevier Ltd. All rights reserved.
doi:10.1016/j.dsr2.2008.02.013

showed a 2-fold increase in primary production rates over the mean in the region (Harris et al., 1997). Despite the relatively higher primary productivity and TChl *a* within these mesoscale features, few data exist regarding how heterotrophic prokaryotes respond in mesoscale eddies.

Heterotrophic bacteria play an important role in the planktonic food web. The amount of organic carbon processed daily by heterotrophic bacteria—the bacterial carbon demand (BCD)—can be comparable to local primary production (Ducklow, 1999). Furthermore, bacteria are key remineralizers of dissolved organic matter (DOM) (Azam and Hodson, 1977; Fuhrman, 1992; Ducklow, 2000), and can play a major role in determining the fate of eddy-stimulated new production. If heterotrophic bacterial activities such as particulate organic carbon (POC) solubilization (Smith et al., 1992) and subsequent POC and dissolved organic carbon (DOC) remineralization are high enough, then a significant fraction of the newly produced organic matter may be regenerated in place (Legendre and Le Fèvre, 1995), thereby minimizing the potential carbon flux of eddies. Little is known about the heterotrophic bacterial response associated with eddy-induced upwelling. Several studies have reported elevated bacterial abundance inside NE Atlantic cold-core eddies (Harris et al., 1997; Lochte and Pfannkuche, 1987; Thyssen et al., 2005) while others have reported no difference in depth-integrated bacterial biomass (BB) inside compared to outside a cyclonic eddy (Gonzalez and Anadon, 2001; Tarran et al., 2001). Even less is known about the associated bacterial production (BP) response in an eddy-induced phytoplankton bloom. Bode et al. (2001) found higher BP rates within a cold-core eddy region near the Canary Islands than in surrounding waters.

The EDdy Dynamics, mixing, Export, and Species composition (EDDIES) project provided a unique opportunity to evaluate the response of heterotrophic prokaryotes to the newly produced organic matter resulting from episodic perturbations in an open-ocean oligotrophic system. In order to characterize the heterotrophic prokaryotic dynamics within the EDDIES program, estimates of BB and BP in two upwelling eddies in the Sargasso Sea were made over two field seasons in 2004 and 2005. Here we compare and contrast the similarities and differences between the heterotrophic bacterial dynamics within and between two eddy types (cyclonic and mode-water) and relative to the phytoplankton community dynamics. We also report findings from a cyclonic eddy that passed over Bermuda Atlantic Time-series Study (BATS) in July 2003.

2. Methods

2.1. Eddy tracking

As part of the EDDIES project, two types of eddies—cyclonic and anticyclonic mode-water—were examined as part of a two-ship operation (see McGillicuddy et al., 2007). The R.V. *Oceanus* provided survey data for several eddies during each year of the study. In an attempt to capture the temporal dynamics in biological and biogeochemical responses to these mesoscale perturbations, a separate set of cruises aboard the R.V. *Weatherbird II* was designed to measure nutrients, vertical flux, primary production and microbial community dynamics. Each eddy type was occupied twice for 10 days within a 1-month period in 2004 and 2005. In 2004, a cyclonic eddy (C1) was surveyed between June 23 and July 2 (C1-1) and again from July 31 to August 9 (C1-2). In 2005, an anticyclonic mode-water eddy, (A4), was surveyed from July 6 to 15 (A4-1) and August 16–25 (A4-2). Near-real-time satellite altimetry (Leben et al., 2002) and shipboard acoustic doppler current profiler (ADCP) data from R.V. *Oceanus* permitted accurate tracking of the eddies throughout the cruises, and allowed for high-resolution sampling across the diameter of each eddy with sampling distances ranging from 10 to 40 km apart aboard R.V. *Weatherbird II* (Fig. 1). The BATS site (31°40′N, 64°10′W) also was sampled during each field season to serve as a control station. To improve comparability, within-eddy data were compared to the BATS summer climatology. All BATS data presented here are available online (http://www.bbsr.edu/cintoo/bats/bats.html). All EDDIES data are also accessible (http://ocb.whoi.edu/jg/dir/OCB/EDDIES/).

2.2. Sample collection

Sample water was collected from the surface 300 m of the ocean via a 24-place CTD rosette equipped with 12-l Niskin bottles containing epoxy-coated springs or from 12-l GoFlo bottles on a Kevlar line. Preliminary experiments showed no significant difference in BP or BB measured in water from GoFlo bottles vs. Niskin bottles. Nitrile gloves were used during sample collection and handling. Only data for the surface 200 m of the ocean are presented in this manuscript, because data below 200 m did not show any appreciable variability.

2.3. Bacterial biomass

2.3.1. Epifluorescence microscopy

Samples for bacterial abundance were collected in 15–50-ml acid-rinsed Falcon tubes, preserved with 0.2-μm-filtered formalin (final concentration 1%) and stored at 4 °C for no more than 48 h before slide preparation. About 5–10-ml samples were filtered onto blackened 0.2-μm polycarbonate filters backed by 0.8-μm mixed ester filters and stained in the dark with 4′,6-diamidino-2-phenylindole (DAPI, final concentration 5 $\mu g\,ml^{-1}$) (Porter and Feig, 1980). Filters were mounted onto slides with Resolve immersion oil (Richard-Allan Scientific) and stored dry at −20 °C until counted on an Olympus BX51 epifluorescence microscope at 1000× magnification. At least 200 cells per slide were counted.

2.3.2. Flow cytometry

Cell abundance also was enumerated using an LSR II flow cytometer (FCM) (BD Biosciences) equipped with a 488-nm excitation laser and standard filter set as described in Campbell (2001) and Marie et al. (1997). This allowed high throughput of samples and was comparable to counts by epifluorescence microscopy (see Section 3). FCM samples were fixed with 0.2-μm-filtered fresh paraformaldehyde (final concentration of 0.5%) and stored at 4 °C for 1–6 h prior to long-term storage in liquid nitrogen (LN) (Vaulot et al., 1989). Cells were stained with SYBR Green I (Molecular Probes) at a final concentration of 1:10,000 (vol:vol) for at least 30 min in the dark and analyzed within 60 min of staining following the protocols of Marie et al. (1997) and Campbell (2001).

The LSR II analytical performance was evaluated for quality control with 3.0-μm Rainbow beads (Spherotech Inc.). Seawater aliquots collected from 80, 100, and 120 m at Hydrostation S (32°10′N, 64°30′W) and stored in LN, were run daily to check the consistency and precision of the system. Flow rate was calibrated by measuring change in weight of 1 ml samples of deionized water before and after 5–10 min flow runs. This flow calibration was assessed before and after each day's run.

Data were acquired in log mode until 20,000 events were recorded, with green fluorescence (GFL) at 200 V set as the discriminator. Gating analysis was performed using FACS Diva software (BD Biosciences). Cell abundance in cells ml^{-1} was calculated from sample flow rates and number of events recorded

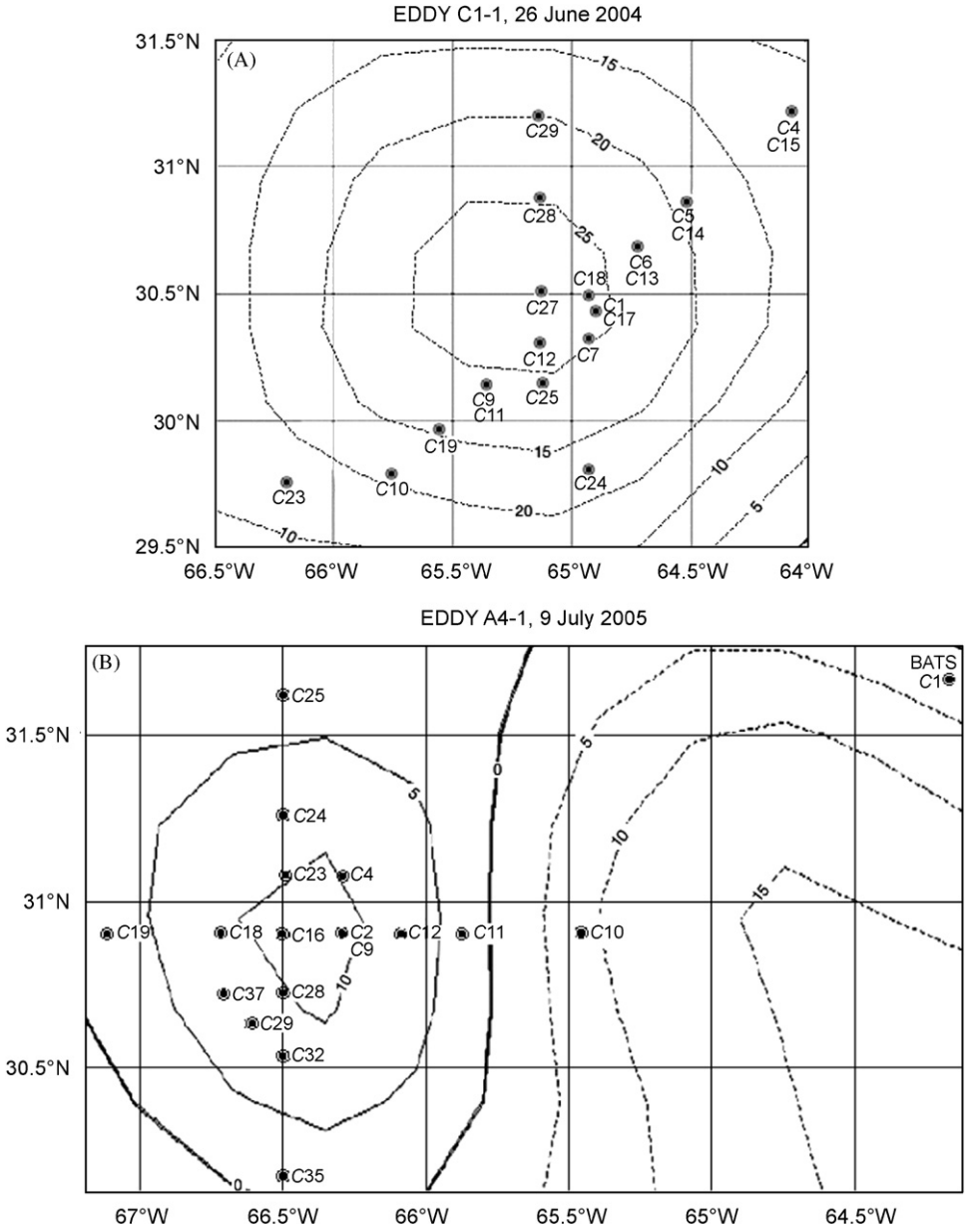

Fig. 1. Cruise tracks for the first occupation of each eddy showing CTD stations where biogeochemical samples were taken aboard R.V. *Weatherbird II*. Solid contours show positive SLA, dashed contours show negative SLA in cm. SLA for each eddy were obtained from merged near-real time satellite altimetry data from Jason, Topex/Poseidon, ERS-2, Envisat and GFO for the first day of each cruise (http://las.aviso.oceanobs.com). *Note*: In panel B, due to eddy propagation, C10 was considered on the eddy periphery by the time it was sampled.

as described in Campbell (2001). BB was estimated from cell abundance using a carbon conversion factor of 10 fg cell^{-1} (Caron et al., 1995; Ducklow, 2000).

2.4. Bacterial production

Heterotrophic BP was estimated by [^{3}H-methyl]-thymidine (^{3}H-TdR) incorporation (Fuhrman and Azam, 1982) using the microcentrifuge method (Smith and Azam, 1992). Briefly, samples for ^{3}H-TdR incorporation incubations were collected directly from Niskin or GoFlo bottles into acid-rinsed 30-ml polycarbonate vials. Duplicate 1.6-ml aliquots were incubated in non-sterile microcentrifuge tubes and were spiked with 10 nM ^{3}H-TdR (specific activities of 91, 88, 86 and 86 Ci mmol^{-1} for cruises C1-1, C1-2, A4-1, A4-2, respectively, Amersham). Non-sterile microtubes were used because previous work with sterile centrifuge tubes demonstrated significant (as much as 50%) reduction in ^{3}H-TdR incorporation when compared to acid-cleaned polycarbonate bottles (unpublished). Linear uptake of ^{3}H-TdR proceeds for at least 4 h throughout the 200-m water column at this site (Carlson et al., 1996); thus, all samples were incubated for 1–4 h in the dark within 2 °C of *in situ* temperature. Incubations were stopped with cold 100% trichloroacetic acid (TCA, 5% final concentration). Blank controls consisted of samples that were killed with TCA prior to addition of radioactive tracer and incubation. DNA was precipitated by pelleting cells in a 4 °C microcentrifuge at 20,800*g* and rinsed with cold 5% TCA, followed by cold 80% ethanol, before resuspension in 1.6-ml scintillation cocktail (Ultima Gold; Smith and Azam, 1992). Radioactivity was analyzed by a Packard Tri-Carb Liquid Scintillation Counter corrected with external standard and quench curve. ^{3}H-TdR uptake rates were converted to

bacterial cell production using the conversion factor 1.63×10^{18} cells mol^{-1} TdR incorporated (Carlson et al., 1996).

2.5. Primary production, total chlorophyll a and pigment analysis

Primary production was measured by ^{14}C-incorporation during *in situ* incubations on a surface-tethered production array as described in US JGOFS BATS methods manual (Knap et al., 1997). Chlorophyll and carotenoid pigment analysis was measured by reverse phase high-performance liquid chromatography (HPLC) also as described in US JGOFS BATS methods manual (Knap et al., 1997). Briefly, 4-l samples were filtered onto 47-mm GF/F filters and stored in LN until onshore analysis at the Center for Hydro-Optics & Remote Sensing, San Diego State University Research Foundation. Pigments were extracted in 90% acetone overnight in the dark at −20 °C before analysis of pigment separation by HPLC. Detection limits were ~1 ng kg^{-1} (Bidigare, 1991). Contribution of individual taxonomic groups to TChl *a* were determined using the algorithm of Letelier et al. (1993) in order to estimate the phytoplankton community structure. While this algorithm was developed for use in the oligotrophic Pacific, it has been successfully applied at BATS (Boyd and Newton, 1999; Steinberg et al., 2001; Sweeney et al., 2003; McGillicuddy et al., 2007); thus, we employed it in this study for comparative purposes.

2.6. BATS cruise B178

The passage of a cold-core cyclonic eddy over BATS during B178 cruise in July 2003 was confirmed by SLA imagery obtained from Jason, Topex/Poseidon, GFO and ERS satellite data (Fig. 2). BP and BB measurements during B178 were performed by the BATS core group according to the US JGOFS BATS methods manual (Knap et al., 1997), which are analogous to the methods described above.

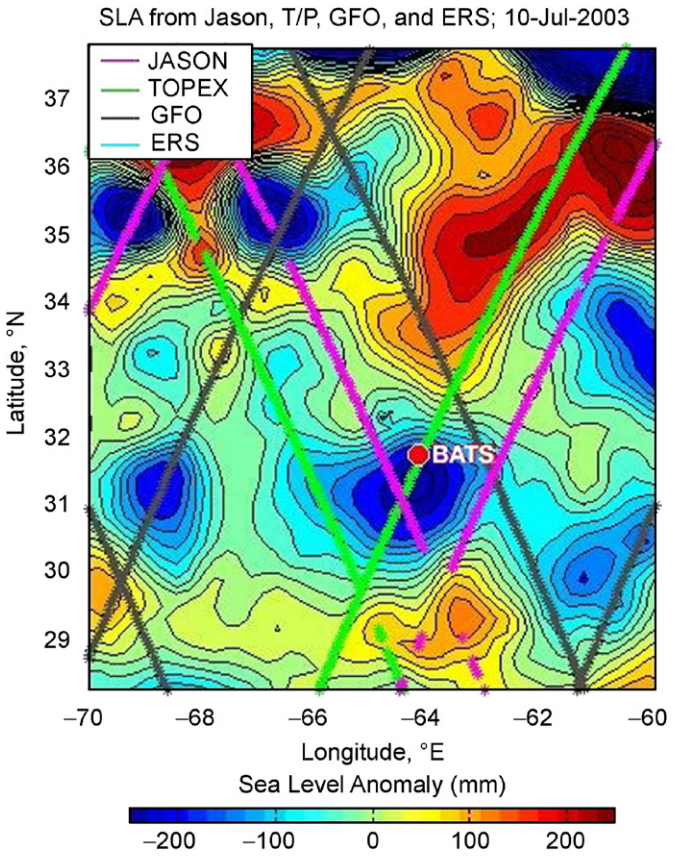

Fig. 2. Sea-level anomaly contours (mm) surrounding BATS on July 10, 2003, determined from Jason, Topex/Poseidon, GFO and ERS satellites. Bold colored diagonal lines are the trajectories of the various satellites. Cold-color and warm-color contours represent negative and positive sea-level anomalies, respectively. Location of BATS sampling station indicated by a red dot.

2.7. Statistical analysis

Rate and stock comparisons between and within eddies (between EC and eddy edges) were tested for significance ($P<0.05$) by 1-way ANOVA followed by paired Student *t*-tests (Student–Newman–Keuls). Pearson product moment correlations were performed to test for association between bacterioplankton parameters and phytoplankton pigment distribution. A significant $r^2>0.5$ ($P<0.05$) was considered a high correlation. Contour plots were created in Ocean Data View (Schlitzer, Ocean Data View, http://www.awi-bremerhaven.de/GEO/ODV, 2004).

3. Results

3.1. Flow cytometry and epifluorescence cell counts

Bacterial abundance for C1-2 was enumerated by epifluorescence direct count microscopy; however, to increase throughput of cell enumeration, we employed FCM for samples collected from other eddy occupations. To ensure that the two methods were comparable, a subset of 12 casts across both eddy types was counted simultaneously by FCM and epifluorescence microscopy. To directly compare both methods of bacterial enumeration, epifluorescence counts were converted to FCM equivalent counts using the following formula:

$$\text{FCM (cells ml}^{-1}) = 0.826 * \text{DAPI (cells ml}^{-1}) + 8194 \quad (1)$$

This formula was based on a linear regression (reduced major axis) of 130 samples spanning 0–300 m from C1 and A4, which were simultaneously counted by FCM and DAPI ($r^2 = 0.76$, $P<0.05$).

3.2. Eddy physical characteristics

3.2.1. Cyclonic eddies B178 and C1

In July 2003, satellite altimetry recorded the passage of a cyclonic eddy through the BATS site, which coincided with sampling during BATS cruise B178. This cold-core eddy, from herein referred to as eddy B178, exhibited a negative SLA of ~25 cm and was approximately 200 km in diameter (Fig. 2).

Cyclonic eddy C1, sampled in 2004, was approximately 160 km in diameter with a negative SLA of ~20 cm (Fig. 1A). Eddy C1 was characterized by a downwelling seasonal thermocline at the center of the eddy (Fig. 3A). The permanent thermocline was upwelled (for details, see McGillicuddy et al., 2007; Li and Hansell, 2008). The downwelling center of the eddy was associated with a low in Chl *a* relative to eddy edges (>25 km from EC), although earlier occupations of the eddy on the survey cruises indicated chlorophyll enhancement at EC (McGillicuddy et al., 2007).

3.2.2. Anticyclonic mode-water eddy A4

Mode-water eddy A4, sampled in 2005, had a diameter of ~200 km and a positive SLA of up to 20 cm (Fig. 1B). The mode-water nature of eddy A4 was demonstrated by the thick lens of 18 °C water associated with upwelling of the seasonal thermocline and downwelling of the permanent thermocline (for details see McGillicuddy et al., 2007). A deep Chl *a* maximum (DCM) was observed at EC between 80 and 110 m (Fig. 3B, Table 1). The A4 Chl

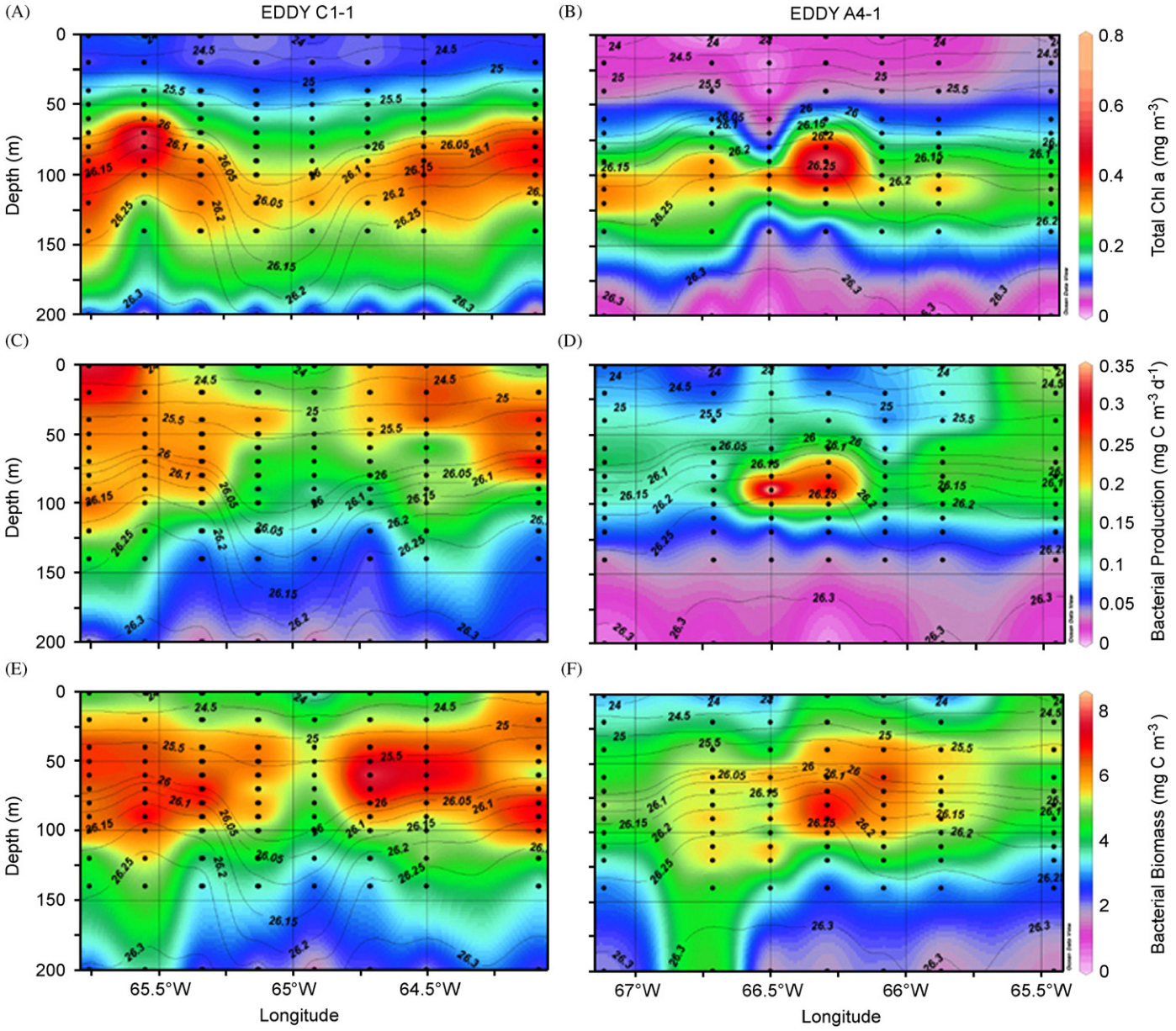

Fig. 3. Contours of total Chl *a* (by HPLC pigment analysis; A and B), BP (C and D) and BB (E and F) in the surface 200 m across a west–east transect of eddies C1 and A4. Black dots are sampling locations. Sigma theta contours (kg m^{-3}) are depicted on each plot.

a max was 1.36 μg L^{-1} along the 26.26 kg m^{-3} isopycnal (~100 m). C1 had a lower Chl *a* signal than A4 overall, with a C1 Chl *a* max of 0.67 μg L^{-1} along the 26.16 kg m^{-3} isopycnal (~70 m).

3.3. Integrated stocks and rates in cyclonic and mode-water eddies

During cruise B178 in July 2003, measurements of ^{3}H-TdR incorporation exceeded typical summer profiles for the region (Fig. 4) and 140-m-integrated microbial production on B178 was 90 mg C m^{-2} d^{-1}, almost 3 times the mean BATS summer climatology (1998–2002) of 38 ± 36 mg C m^{-2} d^{-1} (Fig. 5A). Integrated BB (140 m) during this cruise was also slightly elevated at 835 mg C m^{-2} compared to the BATS summer mean of 714 ± 131 mg C m^{-2} (1993–2003; Fig. 5B). The unusually high BP rates (and to a lesser extent biomass) observed during this cruise were coincident with the passage of cold-core mesoscale perturbation B178 and suggested that heterotrophic microbial processes might be enhanced by the cyclonic eddy. In contrast, 140-m-integrated BP and BB in cyclone C1 and mode-water eddy A4 fell within the range of BATS summer means with no significant difference between them ($P > 0.05$, Fig. 5, Table 1).

3.4. Volumetric rates and concentrations in each eddy

While average integrated parameters for each eddy occupation were not statistically different from BATS climatology, high-resolution horizontal and vertical sampling of BP and BB in the 2004 and 2005 features revealed regular patterns within the surface 200 m of each eddy.

TChl *a*, BP and BB across each eddy demonstrated a high degree of systematic variability with clear differences between the cyclonic and mode-water eddy features. Representative transects of C1 and A4 TChl *a*, BB and BP are depicted in Fig. 3. While only one representative transect per eddy is presented, statistical analyses included all data from all transects (>10 stations per cruise, see Tables 1 and 2). We partitioned each eddy spatially,

Table 1
Integrated values (upper 140 m) for BB, BP, PP, and BCD for eddy edge and center station

Eddy	Eddy occupation	Location	Station (CTD #)	Bacterial biomass ($mg\,C\,m^{-2}$)	Bacterial production ($mg\,C\,m^{-2}\,d^{-1}$)	Primary production ($mg\,C\,m^{-2}\,d^{-1}$)	BCD (= BP/BGE) ($mg\,C\,m^{-2}\,d^{-1}$)	BCD: PP
C1	1 (C1-1)	Edge ($N=10$)	4, 6, 8, 9, 10, 11, 12, 14, 15, 23	791 ± 41 (728–855)	25.0 ± 4.2 (19.1–32.9)	ND	178 ± 30	ND
		Center ($N=3$)	1, 17, 27	568 ± 10 (557–578)	20.5 ± 3.8 (18.2–24.8)	403 ± 119 (307–536)	146 ± 27	0.36
	2 (C1-2)	Edge ($N=3$)	10, 11, 13	806 ± 49 (772–841)	28.1 ± 8.6 (22.0–34.2)	ND	201 ± 61	ND
		Center ($N=1$)	6	793	22.5	594	161	0.27
		BATS	1	671	18.4	ND	131	ND
A4	1 (A4-1)	Edge	4, 10, 11, 12, 19, 23, 24, 25, 32, 35	675 ± 77	15.0 ± 3.1	ND	107 ± 22	ND
		($N=10$)		(556–799)	(12.1–20.6)			
		Center ($N=5$)	2, 16, 28, 29, 37	590 ± 63 (518–673)	16.7 ± 1.7 (14.2–18.3)	273 ± 63 (200–311)	119 ± 12	0.44
		BATS	1	699	9.9	ND	70	ND
	2 (A4-2)	Edge ($N=3$)	10, 16, 17	517 ± 104 (413–621)	19.7 ± 3.6 (17.0–23.8)	ND	141 ± 26	ND
		Center ($N=6$)	1, 5, 20, 25, 26, 34	548 ± 93 (424–691)	22.4 ± 3.7 (17.6–26.8)	688 ± 107 (605–808)	160 ± 26	0.23
BATS summer climatology (BB: 1993–2003; BP: 1999–2002)				714 ± 131 (534–1049)	37.5 ± 25 (12.4–89.5)	426 ± 207	268 ± 179	0.63

Mean ± standard deviation and ranges (in parentheses) of bacterial production and biomass integrated over euphotic zone (140 m) at eddy center and eddy edge stations in each eddy, compared with primary production. BCD is bacterial carbon demand calculated from BP divided by a bacterial efficiency of 14% determined in the Sargasso Sea (see Carlson et al., 1996).

defining *center* as hydrographic stations within 20 km of true EC (point of minimum velocity determined by ADCP) and *periphery/edge* as stations >25 km from true EC.

In C1, the DCM was located between 26.06 and 26.26 $kg\,m^{-3}$ isopycnals, which were lifted into the euphotic zone up to 70 m at the periphery of the eddy, but depressed below 100 m at EC during R.V. *Weatherbird II* occupations. The greatest TChl *a* concentrations were coincident with regions of maximal isopycnal uplift and were enhanced on the periphery of the eddy relative to its center (Fig. 3A). BB and BP in C1 demonstrated a similar trend to TChl *a*, whereby the rates and concentrations were enhanced at the periphery; however, the highest BP rates and BB were located above the DCM (Fig. 3A, C, E).

Mode-water eddy A4 showed a contrasting signature to C1 (Fig. 3B, D, F). A4 demonstrated isopycnal uplift at EC, between 26.1 and 26.3 $kg\,m^{-3}$. The DCM was located within the region of maximal isopycnal uplift, between 26.06 and 26.28 $kg\,m^{-3}$, and was greatest at 100 m at EC. The highest BP was located at EC and coincided with the DCM between 80 and 110 m (Fig. 3D). Elevated BB was located in the vicinity of enhanced TChl *a* and BP but extended laterally from EC (Fig. 3F). Furthermore, maximal BP occurred at a relative minimum in BB at 80–100 m at 66.5°W (Fig. 3D, F).

3.5. Temporal dynamics at eddy centers

During several occupations of ECs, BP and PP estimates were made simultaneously to provide insight regarding the temporal and spatial response of BP compared to PP. Logistical constraints limited the number of in situ PP arrays deployed, so PP measurements were targeted at EC, where eddy-induced stimulation was hypothesized to be greatest due to maximal isopycnal uplift. However, as noted above, maximal isopycnal uplift in C1 was not associated with the EC.

PP arrays conducted at EC of C1 revealed elevated PP rates in the surface 60 m ranging between 5 and 7.5 $mg\,C\,m^{-3}\,d^{-1}$ (Fig. 6A–C). There was little vertical variability in BP profiles within the surface 100 m, with rates remaining $\leqslant 0.3\,mg\,C\,m^{-3}\,d^{-1}$ over the course of repeated occupations (Fig. 6A–C). In contrast, BP and PP estimates in A4 covaried over depth with minimal rates in the surface 40 m and maximal rates occurring between 60 and 80 m (Fig. 6D–F). Maximum volumetric PP rates in A4 were enhanced by 15–20-fold compared to the minimal euphotic zone PP rates (Fig. 6D–F) and were approximately 3–4-fold greater than the maximal PP rates observed in C1 (Fig. 6). The highest volumetric BP rate in A4 ($0.67\,mg\,C\,m^{-3}\,d^{-1}$) was observed at 80 m during the first occupation of the EC and was 2-fold greater than the maximal BP rates observed during C1 (Fig. 6D). However, subsequent occupations of A4 EC revealed maximal BP rates of up to $0.33\,mg\,C\,m^{-3}\,d^{-1}$, similar to maximal rates observed in C1 EC. It is difficult to discern whether the lower BP observed in this second occupation reflects a temporal trend or the substantial submesoscale spatial variability near EC (see Fig. 3 of McGillicuddy et al., 2007).

3.6. Spatial variability of integrated microbial parameters within the cyclonic and anticyclonic eddies

Integrated BP and BB (0–140 m) were determined for the edge and center regions (as described above) for both eddies in the present study (Table 1). While the spatial trends of integrated stocks and rates were generally consistent with those observed for the volumetric measurements (Fig. 3), only BB in C1 showed statistically higher concentrations on eddy edges compared to EC ($P=0.0001$; Table 1). Since substantial vertical and spatial variability was observed in both mesoscale features, integration through the entire euphotic zone potentially masked localized patterns in microbial dynamics between eddies and between regions within eddies (i.e. center vs. edges).

Maximal BB and BP were located above the DCM for all profiles in C1 but within the DCM envelope for A4 (Fig. 3). Mean BP and BB within the DCM envelope were derived by integrating and depth

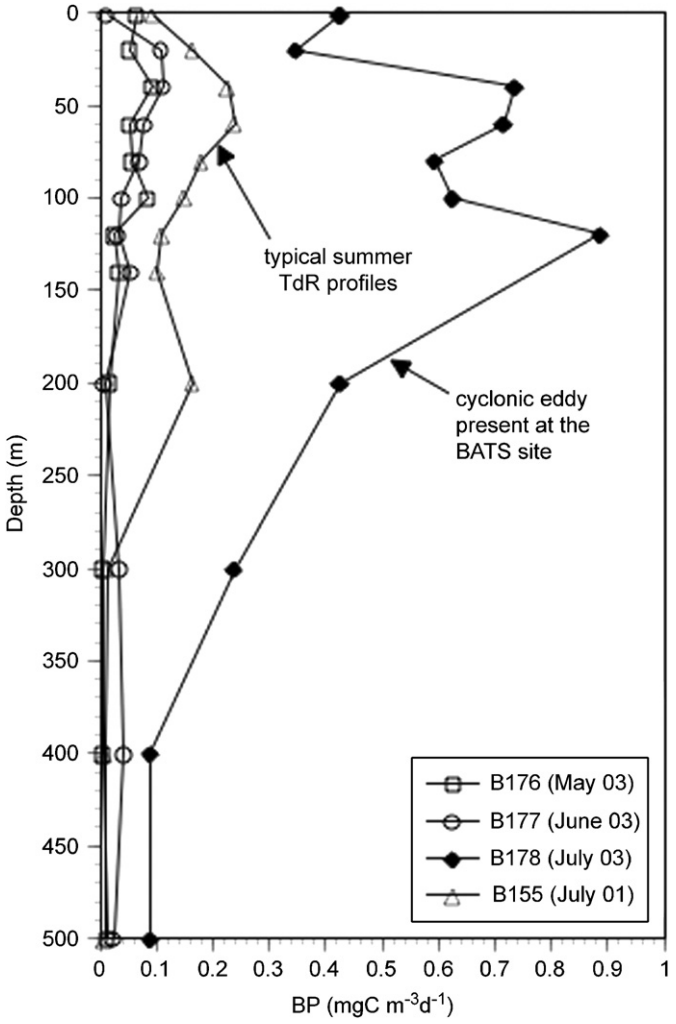

Fig. 4. Profiles of bacterioplankton production rates determined by ^{3}H-TdR incorporation measured at BATS in the presence and absence of a cyclonic eddy. Elevated rates coincided with the passage of cyclonic eddy in July of 2003.

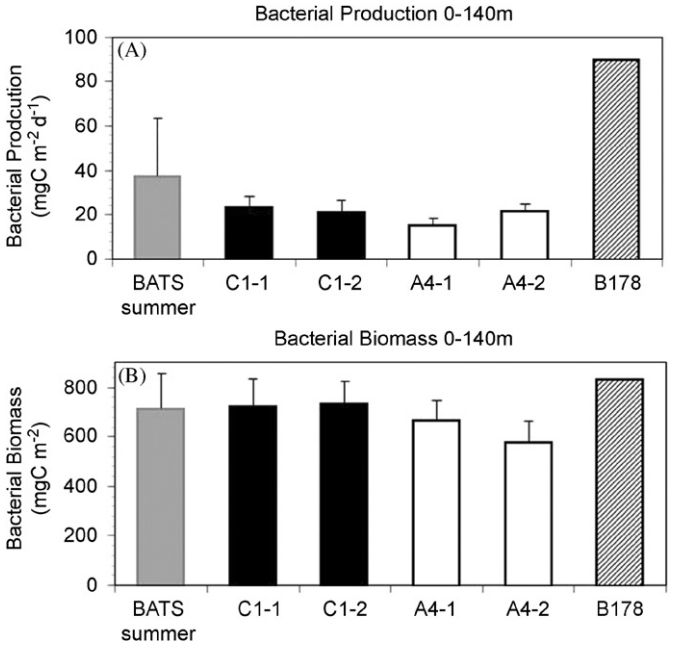

Fig. 5. Mean euphotic zone integrated heterotrophic BP (A) and BB (B) across each eddy and occupation. C1-1 and C1-2: first and second occupations of cyclonic eddy C1. A4-1 and A4-2: first and second occupations of MW eddy A4, respectively. Error bars are 1 SD from mean. BATS summer are means measured over Jun-Aug on BATS cruises during 1998–2002 for BP ($n = 12$) and 1993–2003 for BB ($n = 33$). B178 was the BATS monthly cruise in July that coincided with the passage of a cyclonic eddy.

normalizing between two isopycnal surfaces that bound the DCM (Fig. 7A and B; Table 2). BP rates within the DCM envelope of C1 were not different between EC and edges ($P = 0.0893$), while BB at EC was almost half that at eddy edges ($P = 0.0003$). In contrast, A4 showed a 2.4-fold higher BP rate within the DCM envelope at EC compared to the periphery ($P = 0.0015$; Fig. 7A, Table 2). BB was only slightly higher at EC than at edges in A4 ($P = 0.0045$; Fig. 7B). We also compared mean BB and BP within the DCM envelope to mean values in waters lying above the DCM for each eddy (Table 2). Above the DCM, BP in both eddies remained similar across spatial transects (Fig. 7C), while BB at eddy edges was greater than at EC in cyclone C1 (Fig. 7D). Mean BB and BP in C1 were greatest above the DCM, while BB and BP were greatest within the DCM envelope of A4 (Figs. 3 and 7, Table 2).

3.7. Phytoplankton community structure in C1 and A4

TChl *a* is a general indicator of phytoplankton biomass, and the relative contribution to TChl *a* of various taxonomic groups can be calculated based on accessory pigment composition (Letelier et al., 1993). This analysis provided useful insight into how variations in phytoplankton community structure was related to bacterioplankton variability, since bacterial dynamics appeared to differ significantly with TChl *a* patterns in each eddy.

In the center of C1, the phytoplankton community was similar to mean BATS summer climatology, being dominated by picophytoplankton (*Prochlorococcus* and *Synechococcus* spp., Fig. 8D), while the edge community demonstrated slight enhancement in the relative contribution of prymnesiophytes to TChl *a* compared to BATS mean (Fig. 8A, F, H). A4, on the other hand, showed a substantial shift from the typical BATS summer phytoplankton community with diatoms up to 20% of TChl *a* at EC, which is 7–10 times more than either the eddy edges or BATS summer means (Fig. 8I, L, N).

In an effort to further explain the ecological significance of a decoupling of the BP maximum (BP_{max}) distribution from the DCM in C1 and a tight coupling between the BP_{max} and DCM distributions in A4, Pearson pairwise correlations of BP and BB against the relative abundance of each phytoplankton taxon through the euphotic zone were performed. BP in C1 showed no relationship to TChl *a* (Table 3). Despite the lack of relationship to TChl *a*, BP showed a strong correlation with prymnesiophytes ($r^2 = 0.53$, $P<0.05$) but no other phytoplankton groups in the euphotic zone (Table 3). BB in C1 correlated with *Synechococcus* spp. ($r^2 = 0.51$, $P<0.05$).

In A4, BP positively correlated with TChl *a* over the surface 140 m ($r^2 = 0.52$, $P = 0.0001$; Table 4). In addition, *Synechococcus* spp., prymnesiophytes, diatoms, dinoflagellates and prasinophytes showed strong correlations with BP and BB in A4 with significant Pearson product coefficients >0.5 (Table 4). *Prochlorococcus* abundance by pigment mass showed no relation to BP nor BB ($P>0.05$), and pelagophytes only a weak correlation to BP ($r^2 = 0.33$, $P<0.05$). Prymnesiophytes and diatoms were most correlated with BP and BB (Table 4), with their maxima found at EC, between 80 and 100 m.

4. Discussion

4.1. Normalizing cell counts

FCM counts of all cells correlated well with manual DAPI counts ($r^2 = 0.76$, $P<0.05$), but were typically more conservative

Table 2
Depth normalized means of BP and BB within and above the DCM envelope

Eddy occupation	Isopycnal at DCM ($kg\,m^{-3}$)	DCM envelope ($kg\,m^{-3}$)	Location	DCM envelope		Above DCM	
				BP ($mg\,C\,m^{-3}\,d^{-1}$)	BB ($mg\,C\,m^{-3}$)	BP ($mg\,C\,m^{-3}\,d^{-1}$)	BB ($mg\,C\,m^{-3}$)
C1-1	26.16	26.06–26.26	Eddy edge ($N=10$)	0.16 ± 0.07	5.69 ± 0.73	0.20 ± 0.03	5.74 ± 0.27
			Eddy center ($N=3$)	0.10 ± 0.04	3.23 ± 0.91	0.18 ± 0.07	4.43 ± 0.22
A4-1	26.26	26.16–26.28	Eddy edge ($N=10$)	0.08 ± 0.05	3.88 ± 0.95	0.11 ± 0.03	4.74 ± 0.43
			Eddy center ($N=5$)	0.19 ± 0.03	4.99 ± 0.57	0.09 ± 0.01	3.67 ± 0.72

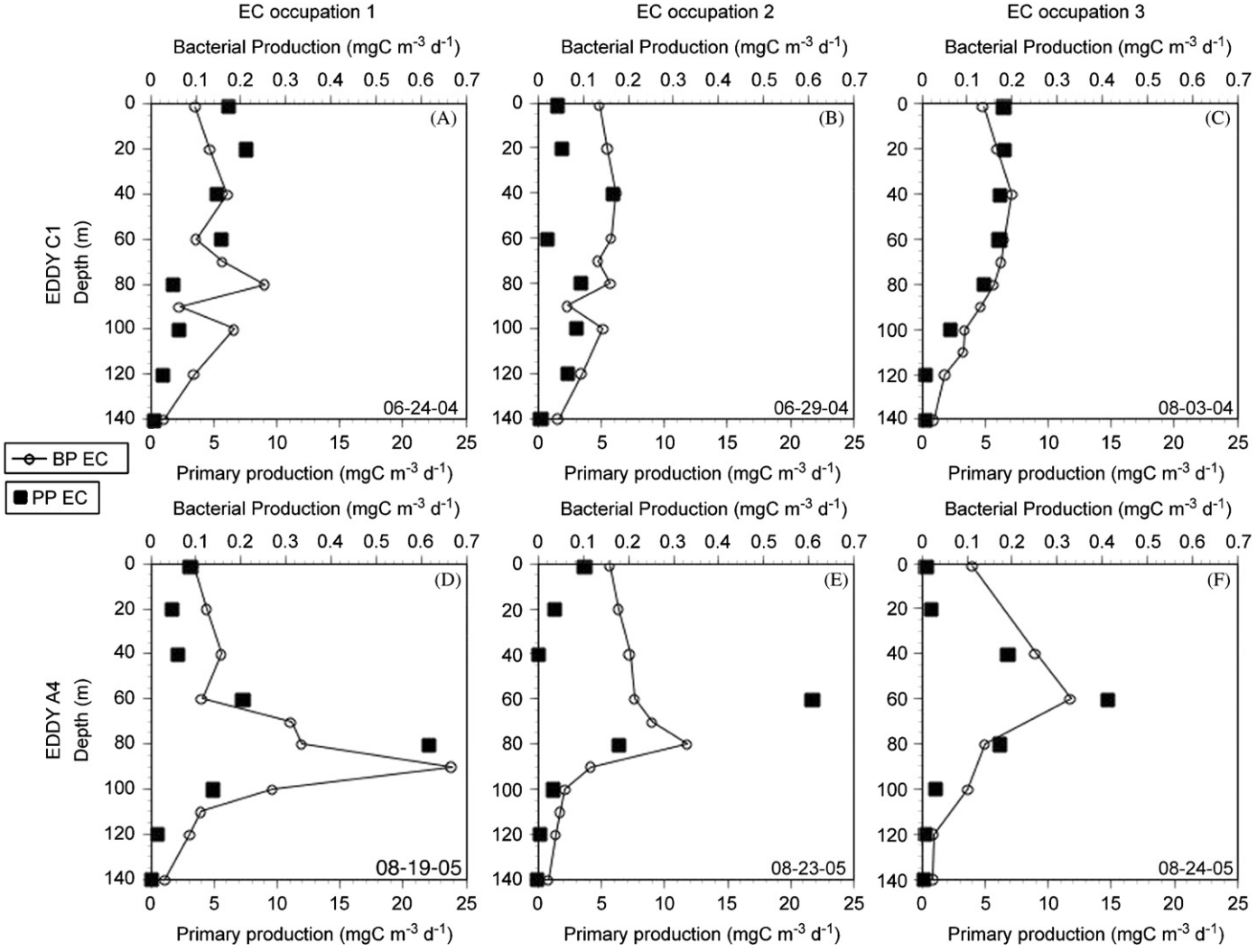

Fig. 6. Primary production and bacterial production profiles over the surface 140 m during several occupations of each eddy center. Filled squares: primary production; open circles with line: bacterial production profile most contiguous in time and space to primary production profile at EC (as determined by ADCP). Dates of EC occupation are indicated in bottom right corner of each panel.

than microscopy counts as has been observed in other studies (Marie et al., 1997; Partensky et al., 1996; Monger and Landry 1993; Vaulot et al., 1989). Cell loss during fixation and freeze/thaw cycle, differences in staining characteristics of SYBR I and DAPI, error in counting debris and inclusion of pigmented cells in total heterotrophic counts by microscopy are some factors that can explain these differences (Marie et al., 1997; Partensky et al., 1996; Monger and Landry, 1993; Vaulot et al., 1989). Since a combination of FCM and epifluorescence microscopy was used to enumerate bacteria, all counts were normalized to the more conservative flow cytometry counts. Normalizing cell counts to FCM data also ensured that only non-pigmented prokaryotes were enumerated, as the FCM allows non-pigmented cells to be distinguished from pigmented cells based on each cell type's fluorescence characteristics (Campbell, 2001).

4.2. Cyclonic eddy B178

The dramatic 3-fold increase in BP over mean summer BP observed at BATS during the passage of cyclonic eddy B178 in July 2003 (Fig. 4 and 5A) was not observed in the EDDIES field program (Fig. 5A). The temporal evolution of the eddy is an important

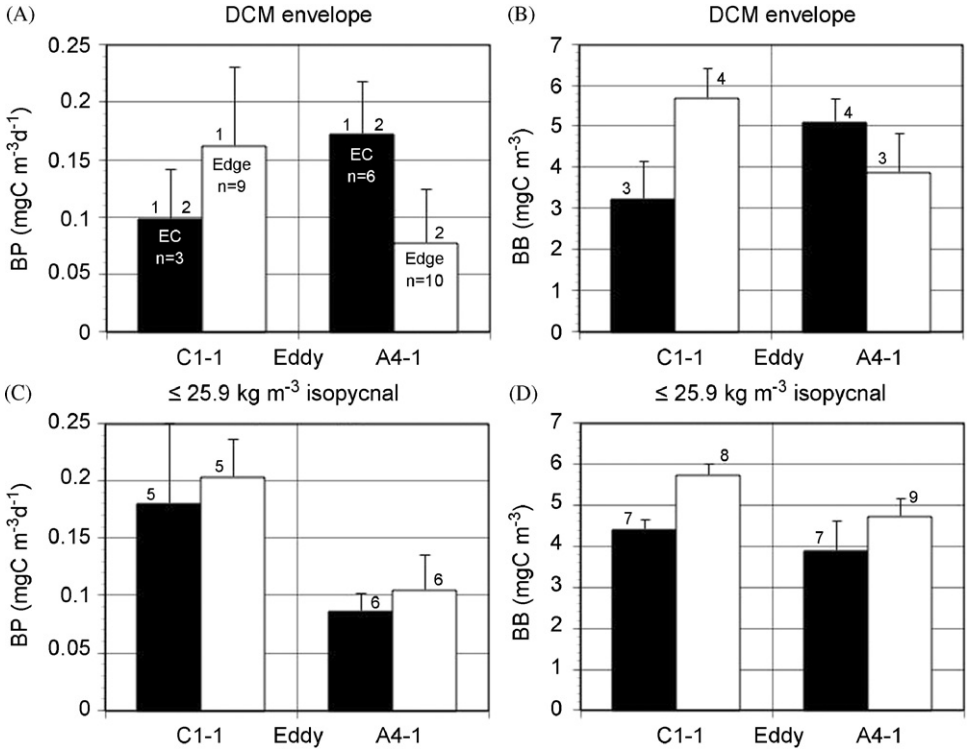

Fig. 7. Spatial variability in BP and BB across eddy C1-1 and A4-1 as a function of eddy region over various depth horizons. BP rates and BB were integrated and depth normalized within the Chl *a* max region or "DCM envelope" (C1-1: 26.06 to 26.26 kg m^{-3}; A4-1: 26.16 and 26.28 kg m^{-3}; panels A, B), and to an isopycnal resting just above the DCM envelope (25.9 kg m^{-3}; panels C, D) in each eddy to account for depth-dependent variations in the DCM. Filled bars are Eddy Center stations, open bars are eddy edge stations. Error bars are 1 SD. Regions that are significantly different by ANOVA and paired *t*-test ($P<0.05$) are marked by differing numbers. Values that are not different from each other share the same number.

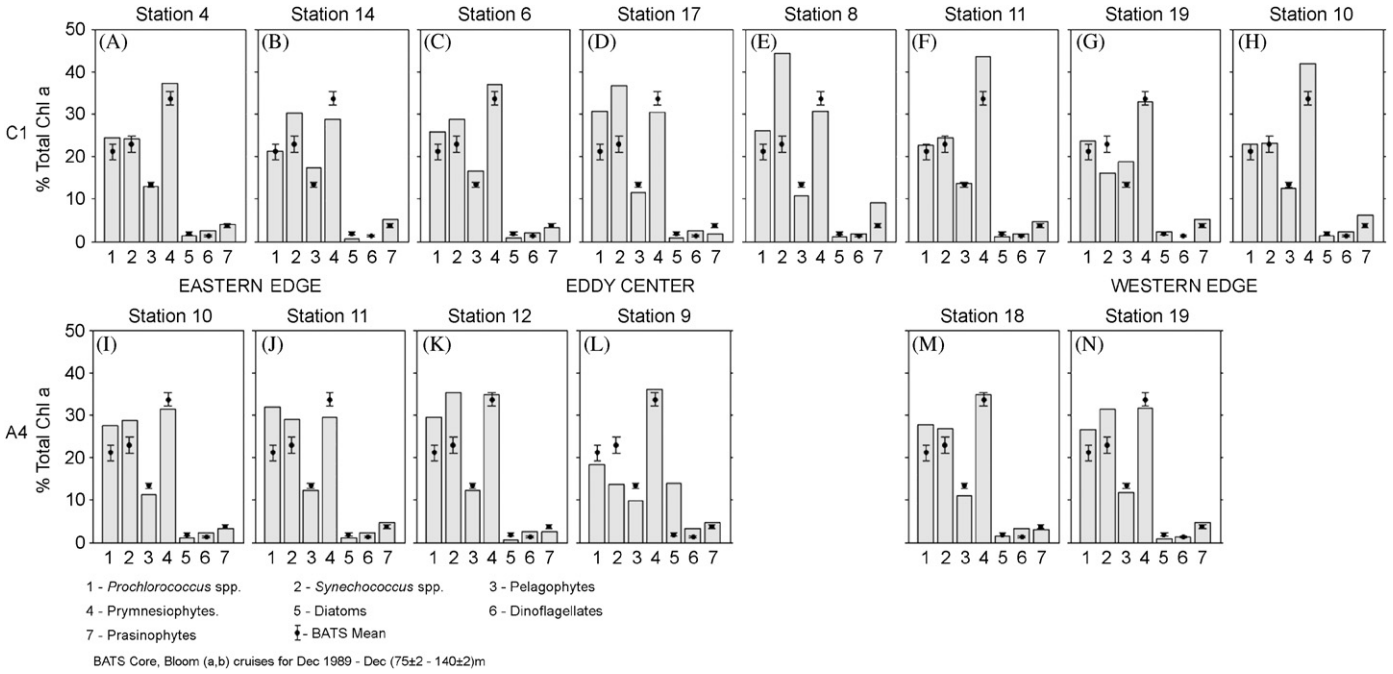

Fig. 8. Phytoplankton community structure integrated over 75–140 m across a transect of each eddy (same transect as shown in Fig. 4) compared to BATS summer means. Community structure assessed from HPLC pigment data using algorithm from Letelier et al. (1993).

consideration when assessing the significance of these perturbations with regard to the biological response (Sweeney et al., 2003). During eddy formation and intensification stages, the flux of new nutrients into the euphotic zone can trigger increased organic matter production (Falkowski et al., 1991; Harris et al., 1997). The altimetric record of eddy B178 suggests it was in a period of SLA intensification when it was sampled (data not shown). Integrated BP within the euphotic zone was almost 3-fold greater than mean background conditions at BATS (Fig. 5A). The local SLA minimum of this cyclonic eddy was located just south of BATS in July 2003,

Table 3
Pairwise correlation analysis of bacterial parameters against phytoplankton community in cyclonic eddy C1

	BB	Total Chl *a* ($mg\,m^{-3}$)	Pro ($mg\,m^{-3}$)	Syn ($mg\,m^{-3}$)	Pelago ($mg\,m^{-3}$)	Prymnesio ($mg\,m^{-3}$)	Diatom ($mg\,m^{-3}$)	Dino ($mg\,m^{-3}$)	Prasino ($mg\,m^{-3}$)
BP ($mg\,C\,m^{-2}\,d^{-1}$)	*0.711*	NS	NS	0.487	NS	*0.528*	0.411	0.412	NS
BB ($mg\,C\,m^{-3}$)	*	0.228	NS	*0.508*	NS	0.454	0.458	NS	NS
Total Chl *a* ($mg\,m^{-3}$)		*	*0.725*	0.426	*0.654*	*0.849*	*0.667*	NS	0.48

Values in table are correlation coefficients (Pearson's product moment, r^2) which are significant, i.e. $P<0.05$. NS means not significant ($P>0.05$). Values in italics represent absolute magnitude of $r^2>0.5$. BP: bacterial production; BB: bacterial biomass; Pro: *Prochlorococcus* spp.; Syn: *Synechococcus* spp.; Pelago: pelagophytes; Prymnesio: prymnesiophytes; Dino: dinoflagellates; Prasino: prasinophytes.

Table 4
Pairwise correlation analysis of bacterial parameters against phytoplankton community in anticyclonic MW eddy A4

	BB	Total Chl *a* ($mg\,m^{-3}$)	Pro ($mg\,m^{-3}$)	Syn ($mg\,m^{-3}$)	Pelago ($mg\,m^{-3}$)	Prymnesio ($mg\,m^{-3}$)	Diatom ($mg\,m^{-3}$)	Dino ($mg\,m^{-3}$)	Prasino ($mg\,m^{-3}$)
BP ($mg\,C\,m^{-2}\,d^{-1}$)	*0.700*	*0.522*	NS	*0.536*	0.33	*0.831*	*0.772*	*0.695*	*0.617*
BB ($mg\,C\,m^{-3}$)	*	0.398	NS	*0.663*	NS	*0.728*	*0.626*	*0.691*	*0.564*
Total Chl *a* ($mg\,m^{-3}$)		*	0.569	0.355	*0.768*	*0.977*	*0.884*	*0.822*	*0.823*

Values are correlation coefficients (Pearson's product moment, r^2), which are significant, i.e. $P<0.05$. NS = no significant relationship ($P>0.05$). Values in italics represents absolute magnitude of $r^2>0.5$. BP: bacterial production; BB: bacterial biomass; Pro: *Prochlorococcus* spp.; Syn: *Synechococcus* spp.; Pelago: pelagophytes; Prymnesio: prymnesiophytes; Dino: dinoflagellates; Prasino: prasinophytes.

while B178 sampling occurred on the northern periphery of the eddy (Fig. 2). The relative enhancement of BP may have resulted from an increase in concentration or flux of organic or inorganic nutrients at the eddy's edges due to physical forcing such as eddy–eddy interaction or horizontal advection. In addition, eddy–wind interactions can have a significant impact upon the magnitude, type and duration of phytoplankton blooms that arise from these features (McGillicuddy et al., 2007). Temporal proximity to eddy intensification stages and resulting bloom conditions may help to explain differences in BB and BP observed during the passage of the cyclonic eddy in July 2003 compared to cyclone C1, as satellite altimetry suggests the latter cyclone was several months old by the time it was sampled (McGillicuddy et al., 2007).

4.3. Cyclonic eddy C1

4.3.1. Physical–biological context

The seasonal thermocline in C1 was downwelling rather than shoaling at EC, suggesting that this cyclonic eddy was in a decay phase during the transects conducted by R.V. *Weatherbird II* (Fig. 3A). A decrease in the fluorescence signal over the course of sampling is further evidence that this eddy was in the later stages of its life cycle (McGillicuddy et al., 2007). This eddy phase may have precluded observations of a biological response to eddy C1 during its intensification stages. In eddy C1, there was a general trend of enhanced TChl *a*, BP and BB at the periphery relative to EC (Fig. 3A, C, E). Similar spatial distributions were observed in the zooplankton biomass (Goldthwait and Steinberg, 2008). Fv/Fm, an indicator of the photosynthetic energy conversion efficiency of phytoplankton cells, as well as Chl *a* concentrations were also at background levels at EC relative to edges (Bibby et al., 2008; Fig. 3).

In addition, a subsurface O_2 deficit coherent with the EC was observed below the euphotic zone (138–140 $\mu mol\,kg^{-1}$ at 250–350 m; see McGillicuddy et al., 2007). If this O_2 deficit was produced locally, it would suggest that a significant fraction of the eddy-induced bloom escaped rapid microbial remineralization and that export occurred prior to the occupation of the eddy (McGillicuddy et al., 2007). Sediment trap-based and ^{234}Thorium-based export measurements (McGillicuddy et al., 2007; Buesseler et al., 2008) were not enhanced, further implying that we sampled the eddy in its decay phase.

Despite the lack of statistical difference between mean BATS summer climatology and euphotic zone integrated bacterial stocks and rates across the cyclonic eddy as a whole (Fig. 5), spatial trends across the eddy were reflected in the volumetric bacterial concentrations and rates, which showed a local minimum at EC (Fig. 3A, C, E) similar to the other biological parameters mentioned above. The local minimum in BP and BB at EC relative to the edge (Fig. 3, Table 1) may be another indication of a prior eddy-induced biological response, which was simply missed during sampling due to eddy decay and/or eddy–wind interactions which decrease eddy-induced upwelling in cyclones (McGillicuddy et al., 2007).

4.3.2. Microbial response and the phytoplankton community

The phytoplankton community in C1 was dominated by picophytoplankton and prymnesiophytes based on pigment analysis (Fig. 8A–H), which is typical of oligotrophic summer conditions in the Sargasso Sea (Durand et al., 2001; Olson et al., 1990; Steinberg et al., 2001). On average, *Prochlorococcus* spp., *Synechococcus* spp., pelagophytes, and prymnesiophytes constituted the largest fractions of TChl *a*, while diatoms, dinoflagellates, and prasinophytes contributed comparatively little to TChl *a* (Fig. 8A–H).

In C1, the DCM at EC was dominated by picophytoplankton, but BP more closely correlated with prymnesiophytes (Table 3) that were located above the DCM (data not shown) and localized at eddy edges where prymnesiophytes dominated the phytoplankton community (Fig. 8). Similarly, Tarran et al. (2001) found that 70% of the phytoplankton standing stocks were comprised of the prymnesiophyte *Coccolithus pelagicus* and other unidentified nanophytoplankton in a Northeast Atlantic cold-core eddy.

Li and Hansell (2008; http://ocb.whoi.edu/jg/dir/OCB/EDDIES/) were not able to resolve any significant removal or production of TOC or TON (on the μM scale) between eddies and BATS. Previous work in the Sargasso Sea has demonstrated that approximately 96–99% of total organic matter is DOM (Hansell and Carlson, 2001); thus for the purposes of this discussion we will refer to this measured pool as DOM (see Hansell, 2002). The lack of DOM

accumulation (μM scale) together with the high correlation of BP with prymnesiophytes ($r^2 = 0.53$; Table 3) is indicative of tight coupling between labile DOM production by this larger eukaryotic group and its rapid utilization by heterotrophic bacterioplankton. Previous studies have reported more rapid microbial utilization of DOM produced by larger eukaryotic phytoplankton compared to that released by picophytoplankton (Tarran et al., 2001; Goldman et al., 1992).

4.4. Mode-water eddy A4

4.4.1. Physical–biological context

In contrast to C1, A4 demonstrated uplift of the seasonal thermocline at EC, which was coherent with enhancement of BP and Chl *a* (Fig. 3B and C). Zooplankton biomass showed significant temporal variation at EC, but was highest when the highest PP was measured during A4-2 (Goldthwait and Steinberg, 2008). An oxygen deficit in A4 EC was observed (~125–130 μmol kg^{-1}), but located deeper (i.e. 800–900 m) than in C1, indicating either an advective entrainment of low O_2 water from a distant source, or implying that a prior bloom and export event had occurred if the oxygen anomaly was locally produced (see McGillicuddy et al., 2007).

In oligotrophic subtropical ecosystems, such as that represented by the BATS site, the DCM is generally observed deeper in the water column than where maximum rates of PP and BP are observed, due to photoadaptation of phytoplankton cells over depth (Michaels and Knap, 1996; Carlson et al., 1996; Steinberg et al., 2001). This scenario is consistent with our observations in C1. In contrast, the maximal values of PP, BP and BB coincided with the DCM envelope in A4, especially at EC. Stochiometric ratios of macronutrient concentrations were similar to C1 with 0.628 μM dissolved nitrate and nitrite (DNN) and 0.029 μM dissolved inorganic phosphate (DIP) at the DCM in A4 compared to 0.627 μM DNN and 0.028 μM DIP in C1 (see Li and Hansell, 2008). Despite similarities in nutrient concentrations, Fv/Fm values were elevated in A4 compared to C1 (A4: 0.457 ± 0.02; C1: 0.439, see Bibby et al., 2008), suggesting greater energy conversion efficiency of the phytoplankton cells in A4.

Another major difference in mode-water eddy A4 compared to cyclonic eddy C1, was that in the center of mode-water eddy A4, diatoms were found at high relative abundance within the DCM (Fig. 8; McGillicuddy et al., 2007), where Chl *a* and primary production were also high (Figs. 3 and 6). In fact, the maximum Chl *a* concentration in A4 (1.36 mg m^{-3}) was eight standard deviations higher than the mean subsurface maximum observed at BATS (McGillicuddy et al., 2007; Steinberg et al., 2001). Wind–eddy interactions in mode-water eddies have been suggested to enhance eddy-upwelling and provide small but steady pulses of nutrient supply to the euphotic zone, which ultimately allows the sustenance of large phytoplankton cells for extended periods (see McGillicuddy et al., 2007; Bibby et al., 2008, for details). This deviation from typical BATS summer phytoplankton community structure in A4 may help explain the higher BP and BB observed at EC than at the periphery within the DCM (Fig. 8A and B).

4.4.2. Microbial response and the phytoplankton community

Within the DCM of A4, integrated BP at EC was significantly higher than at eddy edges, while integrated BB showed less enhancement (Fig. 7A and B). These data indicate variation in specific growth rates across the eddy. The DCM in this eddy was restricted to a very narrow band approximately 20 m thick, between 80 and 100 m along the 26.26 kg m^{-3} isopycnal. The highest BP values, and to a lesser extent BB, were coincident with the region of high Chl *a* and enhanced diatom concentrations at EC (Fig. 3D and F), which is unusual for the Sargasso Sea where maximal primary and secondary production tend to lie above the DCM (Steinberg et al., 2001). In addition, A4 demonstrated strong correlation of BP and BB with all phytoplankton taxa except prochlorophytes and pelagophytes (Table 4), suggesting that the bacterial dynamics in this mode-water eddy were tightly coupled to phytoplankton community dynamics.

Under oligotrophic conditions, the Sargasso Sea is dominated by picoautotrophs (mainly *Prochlorococcus* spp. and *Synechococcus* spp.), which rely mainly on recycled inorganic (Goldman, 1988, 1993) and organic (Palenik et al., 2003; Zehr and Ward, 2002; Zubkov et al., 2003) nutrients produced from the microbial loop. Larger cells such as diatoms have been shown to produce DOM that can be efficiently and rapidly utilized by bacterioplankton (Goldman, 1988, 1993). A high PP measurement at EC during A4-2 (808 mg C m^{-3} d^{-1}) associated with high diatom abundance (Fig. 8) is indicative of periodic pulses in diatom production responsible for the enhanced diatom signal observed during A4. This sustained boom–bust cycle of diatom production could further fuel the microbial loop in the mode-water eddy with increased exudation of labile DOM.

Volumetric rates of BP were enhanced in the DCM of A4 (Fig. 3). There was high correlation between volumetric BP and PP rates observed over vertical profiles, with BP and PP both reaching maximal rates within the DCM envelope (Fig. 6D–F). At first glance, this might indicate that BP was tightly coupled to PP and responding rapidly to freshly produced organic matter from enhanced primary productivity, but we cannot rule out the possibility that both bacterioplankton and phytoplankton were responding to direct inputs of inorganic nutrients. All the evidence presented here—a DCM coincident with the BP/BB max and the depth of maximal PP (Figs. 3 and 6); coincidence of PP and BP vertical profiles at EC (Fig. 6); high correlations of BB/BP with larger phytoplankton pigment biomasses in A4 (Table 4); absence of measurable TOM removal or accumulation in either eddy (Li and Hansell, 2008)—can be explained by a bacterial response to either inorganic nutrients or a secondary response to freshly produced organic matter. Several observations from this study provide insight to assess this problem.

Bacterioplankton may be responding directly to inorganic nutrient pulses. The high surface area to volume ratio of bacterioplankton make them competitive for organic and inorganic substrates (Azam et al., 1983). However, there were differences in BP within the DCM of C1 and A4. BP within the DCM was enhanced in A4 compared to C1 despite similar nutrient concentrations between the two eddies, i.e. C1 (0.627 μM DNN, 0.028 μM DIP) and A4 (0.628 μM DNN, 0.029 μM DIP) (Li and Hansell, 2008). Thus, while both eddies had similar nutrient concentrations within the DCM, the elevated BP response was only observed in A4 within depth horizons coincident with elevated diatom concentrations. Bacterial competition for inorganic nutrients did not prevent net phytoplankton from responding to nutrient inputs in mode-water eddy A4 but the low Fv/Fm ratio and low phytoplankton growth rates in A4 (Bibby et al., 2008) may imply that bacterioplankton impose some competitive limits on diatom growth through the use of inorganic nutrients or are limited by different nutrients such as silica.

The increase in BP at EC coincident with enhanced diatom concentrations and PP (Fig. 6) could be indicative of a transient bacterioplankton response to an increase in bioavailable or labile DOM production. The lack of DOM accumulation seemingly confounds the observed PP enhancement in A4. However, the increase in BP in association with enhanced diatom concentrations and productivity in the absence of net DOM accumulation or removal (on the μM scale) could be explained by the production of

relatively labile DOM that feeds directly into the microbial loop and is turned over rapidly. Similar observations have been documented in the initial phase of seasonal phytoplankton blooms like those described in the Ross Sea (Carlson et al., 1998) where BP increased rapidly coincident with increased PP but net DOM production remained unresolvable.

The direct stimulation of BP by inorganic nutrient inputs or as a secondary response to diatom DOM release are both plausible. However, the discrepancy of the bacterioplankton production response between C1 and A4, despite similar inorganic nutrient concentrations, and the enhanced BP within the diatom-dominated DCM of A4 seemingly suggest a secondary bacterial response to inorganic nutrient input through the production of organic matter via PP and rapid consumption of released DOM.

4.5. Bacterial carbon demand in cyclonic and mode-water eddies

The amount of carbon required to sustain the BP rates observed, i.e. bacterial net production plus respiration, or BCD, is based on the bacterial growth efficiency, which is estimated to be $\approx$14% in the Sargasso Sea (Carlson and Ducklow, 1996). BCD is an indicator of the fraction of organic matter produced via PP that passes through BP. The euphotic zone BCD in cyclonic eddy C1 ranged from 146 to 201 mg C m^{-3} d^{-1} and was greater at eddy edges than at EC, while BCD in mode-water eddy A4 ranged from 107 to 160 mg C m^{-3} d^{-1} and was highest at EC (Table 1). Primary production data are only available for EC in each eddy, thus BCD:PP was only determined for ECs. The fraction of PP processed by bacterioplankton (BCD:PP) ranged from 27% to 36% in eddy C1 and from 23% to 44% in A4 (Table 1), which is comparable to estimates by Carlson et al. (1996) and Ducklow (2000) for the Sargasso Sea, but slightly lower than BCD in the BATS summer record (1999–2002, Table 1) (Steinberg et al., 2001). This would suggest that at the time of these studies, the system was net autotrophic, which is consistent with Mourino-Carballido and McGillicuddy's (2006) findings of general positive net community production (NCP) in cyclones and mode-water eddies. Previous studies have shown a temporal lag between primary production and BP, in which BP may respond to substrates produced by food web processes at a later time from when PP measurements were made (Billen, 1990; Carlson et al., 1996; Ducklow, 1999). However, in this study, PP and BP appear to be highly coherent in mode-water eddy A4 (Fig. 6).

4.6. Summary

Although eddies C1 and A4 did not show enhancement in bacterial dynamics over BATS summer means on the mesoscale, the high-resolution sampling scheme of the EDDIES program allowed us to discern significant submesoscale variability in BP, and to a lesser extent BB, within each eddy. Furthermore, differences in bacterial response between cyclonic and anticyclonic mode-water eddy perturbations were demonstrated, which were closely associated with phytoplankton community structure differences between eddies. It remains unclear whether the differences between BB and BP between cyclones and mode-water eddies is a consistent phenomenon since only two cyclones and one mode-water eddy were surveyed during this study. However, some of the highest NCP estimates for BATS were observed during the passage of a mode-water eddy (Mourino-Carballido and McGillicuddy, 2006). Furthermore, two of the three highest Chl *a* values in the BATS time series were associated with diatom-dominated phytoplankton communities in mode-water eddies (McGillicuddy et al., 2007). Thus, if the coincident spatial positioning of the BP_{max} and the DCM in A4 is related to the community structure, then elevated microbial activity within the DCM rather than above may be a general characteristic of mode-water eddies.

Differences in activity of the total bacterioplankton community across and between the eddies and the covariance of enhanced BP with specific phytoplankton taxa generate questions about variability of the heterotrophic bacterial community structure associated with these trends. In a DMSP-producing coccolithophorid bloom in a North Atlantic cold-core eddy, Gonzalez et al. (2000) found that *Roseobacter*, SAR 86, and SAR 11 were the dominant groups associated with the bloom, all of which were also dominant in non-bloom assemblages. On the other hand, in cyclonic eddies in the lee of the Hawaiian Islands, Becker and Rappé (Benitez-Nelson et al., 2007; Becker and Rappé, 2006) documented community structure shifts in bacterioplankton at EC compared to outside the eddies based on terminal restriction fragment length polymorphism analysis. Differing bacterioplankton community structure between EC and edges could result in differing production rates due to shifts in specific growth rates and bacterial growth efficiencies for each bacterioplankton lineage actively rematerializing substrates. Further investigation of microbial community structure shift in this study is currently underway.

The results presented here demonstrate systematic differences in the bacterial response within and between the cyclonic and mode-water eddies sampled in the Sargasso Sea. Bacterial dynamics were in general very localized and varied on the submesoscale, being associated with isopycnal uplift into the euphotic zone, Chl *a* distribution, phytoplankton community structure, and primary production. The study outlines the complexity of the biological response to mesoscale perturbations and emphasizes the need to incorporate many biological, physical, and chemical factors to explain and model the influence of mesoscale eddies on biogeochemistry in oceanic subtropical gyres.

Acknowledgments

The authors thank Rodney Johnson for his excellent leadership, planning logistics and valuable insights into eddy dynamics. Robert Leben enabled this Lagrangian study by providing near-real-time altimetric data. Thanks also to the captains, crews and scientists of the R.V. *Weatherbird II* and R.V. *Oceanus* for their valuable assistance during the cruises. Our gratitude to the BATS group, Rachel Parsons and Jessica VanLeuven for technical and sampling assistance, Olga Kosnyreva for plotting HPLC-derived community composition, and Charles Trees (CHORS) and NASA for HPLC pigment assays. This manuscript was improved thanks to the valuable contributions of two anonymous reviewers and Claudia Benitez-Nelson. This work was supported by National Science Foundation Biological Oceanography and the Microbial Observatory Programs and NSF Grants OCE 0425615 and MCB0237728 to C.A. Carlson and Chemical and Physical Oceanography to D.J. McGillicuddy.

References

Azam, F., Hodson, R.E., 1977. Size distribution and activity of marine microheterotrophs. Limnology and Oceanography 22, 492–501.

Azam, F., Fenchel, T., Field, J.G., Gray, J.S., Meyer-Reil, L.A., Thingstad, F., 1983. The ecological role of water-column microbes in the sea. Marine Ecology Progress Series 10, 257–263.

Becker, J.W., Rappé, M.S., 2006. Mesoscale to microscale: molecular microbial ecology within cyclonic eddies in the lee of the Hawaiian Islands. Eos Trans AGU 87 (36), Ocean Sciences Meeting Supplement, Abstract OS26E-20.

Benitez-Nelson, C.R., Bidigare, R.R., Dickey, T.D., Landry, M.R., Leonard, C.L., Brown, S.L., Nencioli, F., Rii, Y.M., Maiti, K., Becker, J.W., Bibby, T.S., Black, W., Cai, W.J.,

Carlson, C.A., Chen, F., Kuwahara, V.K., Mahaffey, C., McAndrew, P.M., Quay, P.D., Rappé, M.S., Selph, K.E., Simmons, M.P., Yang, E.J., 2007. Mesoscale eddies drive increased silica export in the Subtropical Pacific Ocean. Science 316, 1017–1021.

Bibby, T.S., Gorbunov, M.Y., Wyman, K.W., Falkowski, P.G., 2008. Photosynthetic community responses to upwelling mesoscale eddies in the subtropical north Atlantic and Pacific Oceans. Deep-Sea Research II, this issue [doi:10.1016/j.dsr2.2008.01.014].

Bidigare, R.R., 1991. Analysis of algal chlorophylls and carotenoids. In: Hurd, D.C., Spencer, D.W. (Eds.), Marine Particles: Analysis and Characterization. Geophysical Monograph, vol. 63. American Geophysical Union, Washington, pp. 119–123.

Billen, G., 1990. Delayed development of bacterioplankton with respect to phytoplankton: a clue to understanding their trophic relationship. Ergebnisse Limnology 34, 191–201.

Bode, A., Barquero, S., Varela, M., Braun, J.G., de Armas, D., 2001. Pelagic bacteria and phytoplankton in oceanic waters near the Canary Islands in summer. Marine Ecology Progress Series 209, 1–17.

Boyd, P.W., Newton, P.P., 1999. Does planktonic community structure determine downward particulate organic carbon flux in different oceanic provinces? Deep-Sea Research I 46, 63–91.

Buesseler, K.O., Lamborg, C., Cai, P., Escoube, R., Johnson, R., Pike, S., Masque, P., McGillicuddy, D., Verdeny, E., 2008. Particle fluxes associated with mesoscale eddies in the Sargasso Sea. Deep-Sea Research II, this issue [doi:10.1016/j.dsr2.2008.02.007].

Campbell, L., 2001. Flow cytometric analysis of autotrophic picoplankton. In: Paul, J.H. (Ed.), Methods in Microbiology: Marine Microbiology. Academic Press, San Diego, CA, pp. 317–341.

Carlson, C.A., Ducklow, H.W., 1996. Growth of bacterioplankton and consumption of dissolved organic carbon in the Sargasso Sea. Aquatic Microbial Ecology 10, 69–85.

Carlson, C.A., Ducklow, H.W., Sleeter, T.D., 1996. Stocks and dynamics of bacterioplankton in the northwestern Sargasso Sea. Deep-Sea Research II 43 (2–3), 491–515.

Carlson, C.A., Ducklow, H.W., Hansell, D.A., Smith, W.O., 1998. Organic carbon partitioning during spring phytoplankton blooms in the Ross Sea Polynya and the Sargasso Sea. Limnology and Oceanography 43, 375–386.

Caron, D.A., Dam, H.G., Kremer, P., Lessard, E.J., Madin, L.P., Malone, T.C., Napp, J.M., Peele, E.R., Roman, M.R., Youngbluth, M.J., 1995. The contribution of microorganisms to particulate carbon and nitrogen in surface waters of the Sargasso Sea near Bermuda. Deep-Sea Research 42 (6), 943–972.

Ducklow, H.W., 1999. The bacterial component of the oceanic euphotic zone. FEMS Microbial Ecology 30, 1–10.

Ducklow, H., 2000. Bacterial production and biomass in the ocean. In: Kirchman, D.L. (Ed.), Microbial Ecology of the Oceans. Wiley-Liss, Inc, New York, pp. 85–120.

Durand, M.D., Olson, R.J., Chisholm, S.W., 2001. Phytoplankton population dynamics at the Bermuda Atlantic Time-series station in the Sargasso Sea. Deep-Sea Research II 48 (8–9), 1983–2004.

Falkowski, P.G., Ziemann, D., Kolber, Z., Bienfang, P.K., 1991. Role of eddy pumping in enhancing primary production in the ocean. Nature 352, 55–59.

Fuhrman, J.A., 1992. Bacterioplankton roles in cycling of organic matter: the microbial food web. In: Falkowski, P.G., Woodhead, A.D. (Eds.), Primary Productivity and Biogeochemical Cycles in the Sea. Plenum Press, New York, pp. 361–383.

Fuhrman, J.A., Azam, F., 1982. Thymidine incorporation as a measure of heterotrophic bacterioplankton production in marine surface waters: evaluation and field results. Marine Biology 66, 109–120.

Goldman, J.C., 1988. Spatial and temporal discontinuities of biological processes in pelagic surface waters. In: Rothschild, B.J. (Ed.), Toward a Theory on Biological–Physical Interactions in the World Ocean. Kluwer Academic, Ducrecht, pp. 273–296.

Goldman, J.C., 1993. Potential role of large oceanic diatoms in new primary production. Deep-Sea Research I 40 (1), 159–168.

Goldman, J.C., Hansell, D.A., Dennet, M.R., 1992. Chemical characterization of three large oceanic diatoms: potential impact on water column chemistry. Marine Ecology Progress Series 88, 257–270.

Goldthwait, S., Steinberg, D.K., 2008. Elevated biomass of mesozooplankton and enhanced fecal pellet flux in cyclonic and mode-water eddies in the Sargasso Sea. Deep-Sea Research II, this issue [doi:10.1016/j.dsr2.2008.01.003].

Gonzalez, J.M., Simó, R., Massana, R., Covert, J.S., Casamayor, E.O., Pedrós-Alió, C., Moran, M.A., 2000. Bacterial community structure associated with a dimethylsulfoniopropionate-producing North Atlantic algal bloom. Applied and Environmental Microbiology 66 (10), 4237–4246.

Gonzalez, N., Anadon, R., 2001. The metabolic balance of the planktonic community in the North Atlantic Subtropical Gyre: the role of mesoscale instabilities. Limnology and Oceanography 46 (4), 946–952.

Hansell, D.A., 2002. DOC in the global ocean carbon cycle. In: Hansell, D.A., Carlson, C.A. (Eds.), Biogeochemistry of Marine Dissolved Organic Matter. Academic Press, San Diego, pp. 685–716.

Hansell, D.A., Carlson, C.A., 2001. Biogeochemistry of total organic carbon and nitrogen in the Sargasso Sea: control by convective overturn. Deep-Sea Research II 48, 1649–1667.

Harris, R.P., Boyd, P., Harbour, D.S., Head, R.N., Pingree, R.D., Pomroy, A.J., 1997. Physical, chemical and biological features of a cyclonic eddy in the region of 61°10′N 19°50′W in the North Atlantic. Deep-Sea Research I 44 (11), 1815–1839.

Jenkins, W.J., Goldman, J.C., 1985. Seasonal oxygen cycling and primary production in the Sargasso Sea. Journal of Marine Research 43, 465–491.

Knap, A.H., Michaels, A.F., Steinberg, D., Bahr, F., Bates, N., Bell, S., Countway, P., Close, A., Doyle, A., Howse, F., Gundersen, K., Johnson, R., Little, R., Orcutt, K., Parsons, R., Rathbun, C., Sanderson, M., Stone, S., 1997. BATS Methods Manual. US JGOFS Planning Office, Woods Hole.

Leben, R.R., Born, G.H., Engebreth, B.R., 2002. Operational altimeter data processing for mesoscale monitoring. Marine Geodesy 25 (1–2), 3–18.

Legendre, L., Le Fèvre, J., 1995. Microbial food webs and the export of biogenic carbon in the oceans. Aquatic Microbial Ecology 9, 69–77.

Letelier, R.M., Bidigare, R.R., Hebel, D.V., Ondrusek, M., Winn, C.D., Karl, D.M., 1993. Temporal variability of phytoplankton community structure based on pigment analysis. Limnology and Oceanography 38 (7), 1420–1437.

Li, Q.P., Hansell, D.A., 2008. Nutrient distribution in baroclinic eddies of the oligotrophic North Atlantic and inferred impacts on biology. Deep-Sea Research, this issue [doi:10.1016/j.dsr2.2008.01.009].

Lochte, K., Pfannkuche, O., 1987. Cyclonic cold-core eddy in the eastern North Atlantic. II. Nutrients, phytoplankton and bacterioplankton. Marine Ecology Progress Series 39, 153–164.

Marie, D., Partensky, F., Jacquet, S., Vaulot, D., 1997. Enumeration and cell cycle analysis of natural populations of marine picoplankton by flow cytometry using the nucleic acid stain SYBR Green I. Applied and Environmental Microbiology 63 (1), 186–193.

McGillicuddy, D.J., Robinson, A.R., Siegel, D.A., Jannasch, H.W., Johnson, R., Dickey, T.D., McNeil, J., Michaels, A.F., Knap, A.H., 1998. Influence of mesoscale eddies on new production in the Sargasso Sea. Nature 394, 263–266.

McGillicuddy, D.J., Johnson, R., Siegel, D.A., Michaels, A.F., Bates, N.R., Knap, A.H., 1999. Mesoscale variations of biogeochemical properties in the Sargasso Sea. Journal of Geophysical Research 104 (C6), 13381–13394.

McGillicuddy, D.J., Anderson, L.A., Bates, N.R., Bibby, T., Buesseler, K.O., Carlson, C.A., Davis, C.S., Ewart, C.S., Falkowski, P.G., Goldthwait, S., Jenkins, W.J., Johnson, R., Kosnyrev, V., Hansell, D.A., Li, Q., Ledwell, J.R., Siegel, D.A., Steinberg, D.K., 2007. Eddy–wind interactions stimulate extraordinary mid-ocean plankton blooms. Science 316, 1021–1026.

Michaels, A.F., Knap, A.H., 1996. Overview of the U.S. JGOFS Bermuda Atlantic Time-series Study and Hydrostation S programs. Deep-Sea Research II 43, 157–198.

Monger, B.C., Landry, M.R., 1993. Flow cytometric analysis of marine bacteria with Hoechst 33342. Applied and Environmental Microbiology 59, 905–911.

Moran, X., Taupier-Letage, I.T., Vazquez-Dominguez, E., Ruiz, S., Arin, L., Raimbault, P., Estrada, M., 2001. Physical–biological coupling in the Algerian Basin (SW Mediterranean): influence of mesoscale instabilities on the biomass and production of phytoplankton and bacterioplankton. Deep-Sea Research I 48 (2), 405–437.

Mourino-Carballido, B., McGillicuddy, D.J., 2006. Mesoscale variability in the metabolic balance of the Sargasso Sea. Limnology and Oceanography 51 (6), 2675–2689.

Olson, R.J., Chisholm, S.W., Zettler, E.R., Altabet, M.A., Dusenberry, J.A., 1990. Spatial and temporal distribution of prochlorophyte picoplankton in the North Atlantic Ocean. Deep-Sea Research I 37 (6), 1033–1051.

Oschlies, A., Garçon, V.C., 1998. Eddy-induced enhancement of primary production in a model of the North Atlantic Ocean. Nature 394, 266–270.

Palenik, B., Brahamsha, B., Larimer, F.W., Land, M., Hauser, L., Lamerdin, J., Regala, W., Allen, E.E., McCarren, J., Paulsen, I., Dufresne, A., Partensky, F., Webb, E.A., Waterbury, J., 2003. The genome of a motile marine Synechococcus. Nature 424, 1001–1002.

Partensky, F., Blanchot, J., Neveux, J., Marie, D., 1996. Vertical structure of picophytoplankton at different trophic sites of the subtropical northeastern Atlantic Ocean. Deep-Sea Research 43, 1191–1213.

Porter, K.G., Feig, Y.S., 1980. The use of DAPI for identifying and counting aquatic microflora. Limnology and Oceanography 25 (5), 943–948.

Schlitzer, R., 2004. Ocean Data View, 〈http://www.awi-bremerhaven.de/GEO/ODV〉.

Siegel, D.A., McGillicuddy, D.J., Fields, E.A., 1999. Mesoscale eddies, satellite altimetry, and new production in the Sargasso Sea. Journal of Geophysical Research 104 (C6), 13359–13380.

Smith, D.C., Azam, F., 1992. A simple, economical method for measuring bacterial protein synthesis rates in seawater using ^{3}H-leucine. Marine Microbial Food Webs 6, 107–114.

Smith, D.C., Simon, M., Alldredge, A.L., Azam, F., 1992. Intense hydrolytic activity on marine aggregates and implications for rapid particle dissolution. Nature 359, 139–142.

Steinberg, D.K., Carlson, C.A., Bates, N.R., Johnson, R.J., Michaels, A.F., Knap, A.H., 2001. Overview of the US JGOFS Bermuda Atlantic Time-series Study (BATS): a decade-scale look at ocean biology and biogeochemistry. Deep-Sea Research II 48, 1405–1447.

Sweeney, E.N., McGillicuddy Jr., D.J., Buesseler, K.O., 2003. Biogeochemical impacts due to mesoscale eddy activity in the Sargasso Sea as measured at the Bermuda Atlantic Time-series Study (BATS). Deep-Sea Research II 50, 3017–3039.

Tarran, G.A., Zubkov, M.V., Sleigh, M.A., Burkill, P.H., Yallop, M., 2001. Microbial community structure and standing stocks in the NE Atlantic in June and July of 1996. Deep-Sea Research II 48 (4–5), 963–985.

Thyssen, M., Lefevre, D., Caniaux, G., Ras, J., Fernandez, C.I., Denis, M., 2005. Spatial distribution of heterotrophic bacteria in the northeast Atlantic (POMME study area) during spring 2001. Journal of Geophysical Research 110 (C07S16).

Vaulot, D., Courties, C., Partensky, F., 1989. A simple method to preserve oceanic phytoplankton for flow cytometric analyses. Cytometry 10, 629–635.

Zehr, J., Ward, B.B., 2002. Nitrogen cycling in the ocean: new perspectives on processes and paradigms. Applied and Environmental Microbiology 68 (3), 1015–1024.

Zubkov, M.V., Fuchs, B.M., Tarran, G.L., Burkill, P.H., Amann, R., 2003. High rate of uptake of organic nitrogen compounds by *Prochlorococcus* cyanobacteria as a key to their dominance in oligotrophic oceanic waters. Applied and Environmental Microbiology 69 (2), 1299–1304.